Multiferroic epitaxial Pb (Fe 1 2 Nb 1 2) O 3 thin films: A relaxor ferroelectric/weak ferromagnet with a variable structure

Li Yan, Jiefang Li, Carlos Suchicital, and D. Viehland

Citation: Applied Physics Letters **89**, 132913 (2006); doi: 10.1063/1.2357926
View online: http://dx.doi.org/10.1063/1.2357926
View Table of Contents: http://scitation.aip.org/content/aip/journal/apl/89/13?ver=pdfcov
Published by the AIP Publishing

Multiferroic epitaxial $Pb(Fe_{1/2}Nb_{1/2})O_3$ thin films: A relaxor ferroelectric/weak ferromagnet with a variable structure

Li Yan,[a] Jiefang Li, Carlos Suchicital, and D. Viehland
Department of Materials Science and Engineering, Virginia Tech, Blacksburg, Virginia 24061

(Received 16 June 2006; accepted 17 August 2006; published online 29 September 2006)

The authors report the structural, ferroelectric, and ferromagnetic properties of $Pb(Fe_{1/2}Nb_{1/2})O_3$ epitaxial thin layers grown on (001), (110), and (111) $SrTiO_3$ substrates by pulsed-laser deposition; films were of sufficient resistivity to enable high-field *P-E* measurements. Findings are as follows: epitaxial strain results in (i) a dramatic increase in the spontaneous polarization P_s; (ii) a lattice structure that is dependent on substrate orientation; (iii) a slim-loop *P-E* response and relaxor ferroelectric characteristics in the dielectric constant, both of which are nearly independent of crystallographic orientation; and (iv) a weak ferromagnetic moment, which is dependent on epitaxial mismatch. © *2006 American Institute of Physics*. [DOI: 10.1063/1.2357926]

Lead iron niobate, $Pb(Fe_{1/2}Nb_{1/2})O_3$ (PFN), was discovered by Smolenskii *et al.* in the 1950s.[1] It is a multiferroic transforming from a paraelectric (cubic) phase to a ferroelectric (rhombohedral) one at a Curie temperature of 385 K,[1,2] concurrently from a paramagnetic state to antiferromagnetic (AFM) spin-ordered one at a Néel temperature of 143 K,[3] and subsequently undergoing a secondary AFM→AFM transition at 19 K.[4,5] The room temperature lattice structure of PFN single crystals is rhombohedral, with lattice parameters of a_r=4.0123 Å (or 4.058 Å) and α_r=89.89°.[1,3,6,7] It is a mixed *B*-site cation perovskite and accordingly could be anticipated to have relaxor ferroelectric characteristics similar to $Pb(Zn_{1/3}Nb_{2/3})O_3$, such as slim-loop polarization (*P-E*) characteristics[8] and a polarization dynamics that scale to a Vogel-Fulcher or stretched exponential relations.[9]

The dielectric, ferroelectric, and magnetic properties of PFN bulk single crystals and ceramics have been reported. The maximum polarization is only ~10 $\mu C/cm^2$,[10] the *P-E* response is "nonsquare" yet hysteretic, the dielectric breakdown field is low, and the weak-field dielectric loss (or tan δ) factors are quite high. These limited dielectric and ferroelectric properties of bulk crystals and ceramics are believed to reflect inferior dielectric insulation, presumptively attributed to conductive losses via valence band hopping due to $Fe^{+2} \rightarrow Fe^{+3}$. In addition, the induced magnetization of PFN single crystals at 80 K has been reported to be <100 emu/cm^3 under a magnetic field of $H=10^5$ Oe.[6] Unlike a normal AFM, at lower fields of $H<2\times10^4$ Oe, the induced magnetization was not linear with applied *H*; rather, the *M-H* response was slim loop with a saturation magnetization of $M_s \approx 20$ emu/cm^3, indicative of a weak ferromagnetism with no remanence.

Nonepitaxial thin layers of PFN have been previously prepared by sol-gel[11,12] and pulsed-laser deposition (PLD).[13,14] Superior ferroelectric properties were reported in both cases, relative to bulk crystals and ceramics. Sedlar and Sayer[11] found the maximum polarization to be P_m =24 $\mu C/cm^2$ for sol-gel films, and Gao *et al.*[13] reported a value of P_m=22 $\mu C/cm^2$ for PLD films deposited on $La_{0.7}Sr_{0.3}MnO_3/Si(001)$. However, epitaxial PFN films have yet to be prepared and studied. The ferroelectric[15] and ferromagnetic[16] properties of epitaxial thin layers with large stictions have been shown to be significantly altered by epitaxial strain. An in-plane compressive stress can result in an increase of the out-of-plane remanent polarization; however, biaxial tension will result in decreased out-of-plane polarization. For example, the apparent value of P_s was increased (by approximately ten times) to 60 $\mu C/cm^2$ for [001]-epitaxial $BiFeO_3$ (BFO) thin layers grown on $SrRuO_3/SrTiO_3$ (or SR0/STO) electrode/substrate, relative to [001]-oriented bulk crystals;[17] also, for epitaxial $BaTiO_3$ thin layers, P_s has been found to be increased to 80 $\mu C/cm^2$.[18] Furthermore, epitaxial stress results in important structural and magnetic property changes, relative to those of corresponding bulk crystals. For example, (001), (101), and (111) epitaxial BFO thin layers are tetragonal (*T*) monoclinic *A* (M_A), and *R*, respectively.[15]

Here, we report the structural, ferroelectric, and ferromagnetic properties of epitaxial PFN thin layers grown on $SrRuO_3/SrTiO_3$ by PLD that were quite resistive. In order to ensure the stoichiometric ratio of different ions, we fabricated PFN targets using a single-step solid-state reaction method. First, powders of PbO, Fe_2O_3, and Nb_2O_5 of >99.9% purity were stoichiometrically mixed with a 5% excess of PbO and then milled, calcined at 850 °C for 3 h; remilled, powders sieved, targets pressed, and subsequently sintered at 920 °C for 3 h in a PbO-rich atmosphere. Epitaxial thin layers of PFN were then deposited on STO substrates with (and without) a SRO buffer (electrode) layer by PLD. The energy density of the KrF laser (Lambda 305i) was 1.2 J/cm^2, and the distance between target and substrate was 6 cm. A bottom SRO electrode was first deposited on the STO substrate at 650 °C at a growth rate 0.7 nm/min. Films of PFN were then deposited at 630 °C at a growth rate of 10 nm/min to an average layer thickness of ~200 nm. A top gold electrode was then deposited by sputtering. The crystal structure of the films was measured using a Philips X'pert system equipped with a two-bounce hybrid monochromator, an open three-circle Eulerian cradle, and a domed hot stage. Mesh and line scans were both obtained to confirm the epitaxial film's orientation and phase purity. All measurements were referenced to the reciprocal lattice unit of $a^*=2\pi/a$ =1.635 Å^{-1}. The following properties of the films were measured using the respective measurement systems: the polar-

[a]Electronic mail: lyan@vt.edu

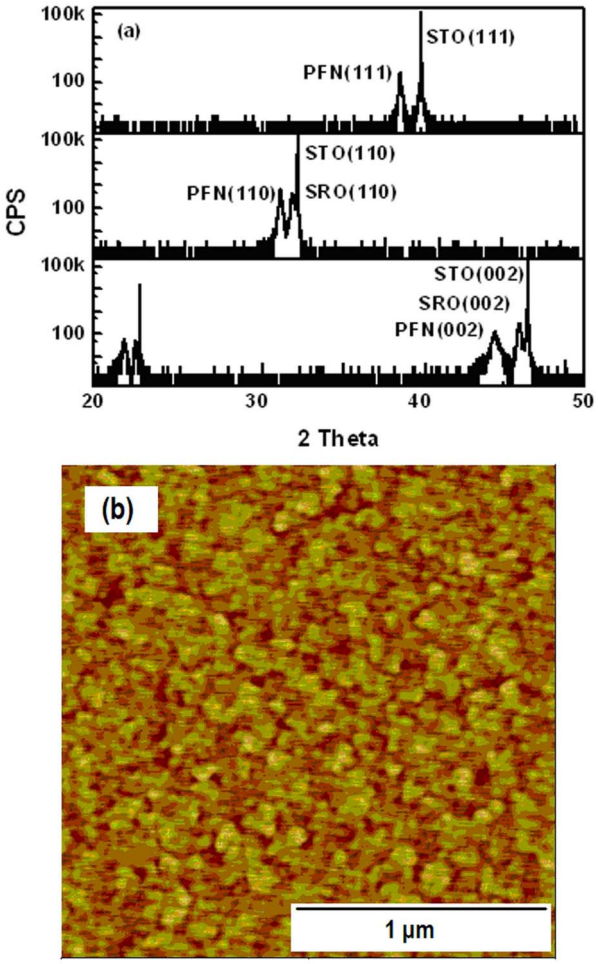

FIG. 1. (Color online) XRD and AFM results of PFN thin film. (a) Line scan over wide angles, demonstrating phase purity and good epitaxy; and (b) AFM image demonstrating the morphology of a typical PFN film.

ization and resistivity (Radiant Technology precision workstation and Signatone probe station), magnetization (Quantum Design superconducting quantum interference device), and morphology (Veeco DI 3100a).

First, we measured the resistivity (ρ) of our PFN thin layers. We achieved room temperature values on order of $\rho > 10^9\ \Omega$ cm, depending on thickness and deposition conditions. The thin layers which we studied in this investigation had thicknesses of about 200 nm and resistivities of $\rho > 10^{10}\ \Omega$ cm, which are considerably higher than reports for bulk crystals/ceramics and nonepitaxial thin films. Such high insulation resistance proved effective in sustaining higher electric fields, preventing dielectric breakdown, and allowing investigation of polarization reversal.

Next, the structure and surface morphology of the PFN thin films were measured by x-ray diffraction (XRD) and atomic force microscopy, respectively. XRD line scans of PFN thin layers grown on (001), (110), and (111) STO substrates buffered with a SRO thin layer are shown in Fig. 1(a). From this figure, we established that all of our thin layers were phase-pure perovskite and also epitaxial. Mesh scans (not shown) demonstrated good epitaxy on the substrate. The atomic force image shown in Fig. 1(b) reveals a surface roughness of ~10 nm and an average crystallite size of ~150 nm.

We summarize how the room temperature lattice structure of PFN films depends on orientation, as given in Table I. We found that (001) oriented films had a tetragonal (T) structure with lattice parameters of a_t=4.010 Å (in plane) and c_t=4.071 Å (out of plane); that (110) oriented films had an orthorhombic (O) structure with a doubled unit cell and lattice parameters of a_o=5.696 Å (in plane), b_o=5.670 Å (out of plane), and c_o=4.025 Å (in plane); and that (111) oriented films had a rhombohedral (R) structure with lattice parameters of a_r=4.027 Å (out of plane) and γ=89.98°, which is similar to that previously reported for bulk PFN single crystals which is the R phase with $a_r=b_r=c_r$.[6] The lattice mismatch (ε) between substrate and film can be calculated as $\varepsilon=[(a_{\text{film}}-a_{\text{substrate}})/a_{\text{substrate}}]\times 100\%$. The lattice parameter of the STO substrate was $a_{\text{substrate}}$=3.905 Å. Using our respective values for the in-plane lattice parameter of the variously oriented films, we can estimate the epitaxial lattice mismatches as summarized in Table I: $\varepsilon_{(001)}$=4.26%, $\varepsilon_{(110)}$=3.20%, and $\varepsilon_{(111)}$=3.17%. In addition, the values of full width half maximum (FWHM) are also summarized in Table I. It can be seen that the FHWM was larger for the (001) films (0.16°) than for either the (110) or (111) films (0.05°–0.06°). The results for the eptiaxial mismatch and the peak broadness are consistent with each other for the various orientations, revealing that they are largest for the (001) film and notably less for the (110) and (111) which are nearly equivalent to each other.

Figure 2(a) shows the P-E response of PFN thin layers with out-of-plane orientations of (001), (110), and (111). The maximum polarization can be seen to achieve values approaching 70 μC/cm^2 under electric fields of $E > 190$ kV/cm, which is much larger (nine times and three times) than that previously reported (bulk and thin layers, respectively). The remanent polarizations of the (001), (110), and (111) oriented thin layers were 18, 17, and 13 μC/cm^2, respectively; correspondingly, the coercive fields were 16, 16, and 15 kV/mm, respectively. It is important to note that the induced polarization under a constant field level was nearly equivalent for all three orientations. For example, consider E=125 kV/cm, the induced polarizations were 56, 54, and 47 μC/cm^2 for (001), (110), and (111) oriented films. These results clearly demonstrate that the polarization

TABLE I. Lattice structure and lattice constant of (001), (110), and (111) oriented PFN thin films.

Substrate	a (Å)	b (Å)	c (Å)	γ (deg)	Structure	FWHM (deg)	ε (%)
(001) STO	4.010	4.010	4.071	90	Tetragonal	0.16	4.26
(110) STO	5.696	5.670	4.025	90	Orthorhombic	0.06	3.20
(111) STO	4.027	4.027	4.027	89.98	Rhombohedral	0.05	3.17

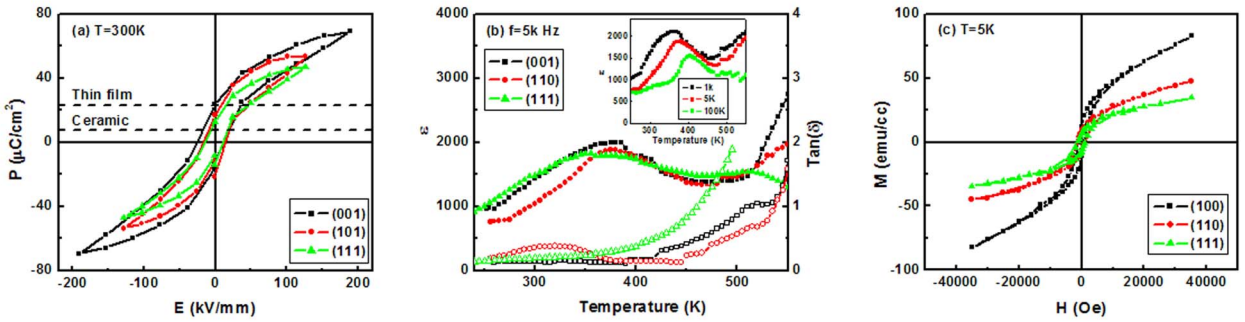

FIG. 2. (Color online) Polarization and weak-field dielectric constant of variously oriented PFN films. (a) Polarization as a function of E at 300 K, where data for nonepitaxial films and bulk ceramics are illustrated by dashed line; (b) complex dielectric constant as a function of temperature taken at a measurement frequency of 1 kHz for variously oriented films, where the inset shows that of (110) films for various frequencies; and (c) magnetization as a function of H at 5 K.

of PFN epitaxial thin layers is nearly independent of orientation. It is not anisotropic, but rather nearly isotropic: in spite of the fact that the crystal structure and lattice parameters were different.

We then measured the temperature dependence of the dielectric constant for the various oriented films, as given in Fig. 2(b). The value of the dielectric constant ($\varepsilon \approx 1000$ at 300 K and $\varepsilon \approx 2000$ at 400 K) and its maximum ($T_C \approx 400$ K) can be seen to be nearly constant for the various orientations. This value of $T_C \approx 400$ K is consistent with prior investigations of bulk crystals/ceramics,[13] although the value of ε is notably smaller for the thin layers than reported for bulk PFN. In addition, the temperature dependence of ε revealed a strongly diffuse or broadened phase transition for the variously oriented films. Furthermore, the inset of Fig. 2(b) shows ε as a function of temperature taken at various frequencies for a (110) oriented film. These results demonstrate relaxor ferroelectric characteristics, consistent with the slip-loop-like P-E response that was nonsquare. The dielectric loss factor is on the level of about 0.1–0.3 at room temperature and notably increased with increasing temperature. This result confirms prior reports of high dielectric loss in PFN. It is relevant to note that nearly identical relaxor responses were found in films of T, O, and R structures, i.e., the relaxor state is invariant to changes in apparent phase stability.

Finally, we measured the in-plane M-H response of PFN(150 nm)/STO, as given in Fig. 2(c). The induced magnetization was on the order of 30–80 emu/cm^3 at a field level of $H \approx 30$–40 kOe, consistent with prior reports.[6,19] Our M-H data are consistent with an AFM spin order with a weak ferromagnetism, and furthermore, the value of M's is close to that reported for the homogeneous (commensurate) spin state of BFO.[17] In the M-H responses, we noticed that there was a general trend between the induced magnetization and the epitaxial mismatch between the film and substrate: the higher the mismatch, the larger the magnetization.

In summary, we have deposited epitaxial PFN thin layers on (001), (110), and (111) SRO/STO. Our results demonstrate a relaxor ferroelectric state, whose crystal lattice structure and lattice parameters are variable to epitaxial mismatch but whose polarization and dielectric constant are nearly independent. Specifically, we find that (i) the structure is dependent on the substrate orientation, (001), (110), and (111) films are T, O, and R, respectively; (ii) the value of $P_s = 70\ \mu\text{C/cm}^2$ is notably larger than that of bulk crystals, nearly independent of film orientation and lattice structure, and possesses slim P-E responses; (iii) the dielectric constant exhibits a diffuse phase transformation and relaxor characteristics, with a Curie temperature of ~400 K; and (iv) a weak ferromagnetic moment, where the moment is seemingly dependent on epitaxial mismatch.

This research work was supported by the Department of Energy and by Air Force Office of Scientific Research.

[1] G. A. Smolenskii, A. Agranovskaya, S. N. Popov, and V. A. Isupov, Sov. Phys. Tech. Phys. **28**, 2152 (1958).
[2] G. L. Platonov, L. A. Drobyshev, Y. Y. Tomashpolskii, and Y. N. Venevtsev, Sov. Phys. Crystallogr. **14**, 692 (1970).
[3] V. A. Vokov, I. E. Mylnikova, and G. A. Smolenskii, Sov. Phys. JETP **15**, 447 (1962).
[4] T. Watanabe and K. Kohn, Phase Transitions **15**, 57 (1989).
[5] V. V. Bhat, K. V. Ramanujachary, S. E. Lofland, and A. M. Umarji, J. Magn. Magn. Mater. **280**, 221 (2004).
[6] Y. Yang, J. M. Liu, H. B. Huang, W. Q. Zou, P. Bao, and Z. G. Liu, Phys. Rev. B **70**, 132101 (2004).
[7] Y. Yang, S. T. Zhang, H. B. Huang, Y. F. Chen, Z. G. Liu, and J. M. Liu, Mater. Lett. **59**, 1767 (2005).
[8] D. Viehland, J. Appl. Phys. **88**, 4794 (2000).
[9] D. Viehland, S. J. Jang, L. E. Cross, and M. Wuttig, J. Appl. Phys. **69**, 414 (1991).
[10] O. Raymond, R. Font, N. Suárez-Almodovar, J. Portelles, and J. M. Siqueiros, J. Appl. Phys. **97**, 084107 (2005).
[11] M. Sedlar and M. Sayer, J. Appl. Phys. **80**, 372 (1996).
[12] Q. Lin, G. Yi, and D. Barber, Mater. Lett. **38**, 239 (1999).
[13] X. S. Gao, X. Y. Chen, J. Yin, J. Wu, Z. G. Liu, and M. Wang, J. Mater. Sci. **35**, 5421 (2000).
[14] X. R. Wang, S. S. Fan, Q. Q. Li, B. L. Gu, and X. W. Zhang, Jpn. J. Appl. Phys., Part 2 **35**, L1002 (1996).
[15] J. Li, J. Wang, M. Wuttig, R. Ramesh, N. Wang, B. Ruette, A. P. Pyatakov, A. K. Zvezdin, and D. Viehland, Appl. Phys. Lett. **25**, 5261 (2004).
[16] F. Bai, J. Wang, M. Wuttig, J. Li, N. Wang, A. P. Pyatakov, A. K. Zvezdin, L. E. Cross, and D. Viehland, Appl. Phys. Lett. **86**, 032511 (2005).
[17] J. Wang, J. B. Neaton, H. Zheng, V. Nagarajan, S. B. Ogale, B. Liu, D. Viehland, V. Vaithyanathan, D. G. Schlom, U. V. Waghmare, N. A. Spaldin, K. M. Rabe, M. Wuttig, and R. Ramesh, Science **299**, 1719 (2003).
[18] K. J. Choi, M. Biegalski, Y. L. Li, A. Sharan, J. Schubert, R. Uecker, P. Reiche, Y. B. Chen, X. Q. Pan, V. Gopalan, L. Q. Chen, D. G. Schlom, and C. B. Eom, Science **306**, 1005 (2004).
[19] S. B. Majumder, S. Bhattacharyya, R. S. Katiyar, A. Manivannan, P. Dutta, and M. S. Seehra, J. Appl. Phys. **99**, 024108 (2006).